

A new drug-loading technique with high efficiency and sustained-releasing ability via the Pickering emulsion interfacial assembly of temperature/pH-sensitive nanogels



Guofeng Zhou^{a,c,1,3}, Yanbing Zhao^{a,b,*}, Jindong Hu^{b,2}, Liang Shen^{a,1}, Wei Liu^{a,b,1,2}, Xiangliang Yang^{a,b,1,2}

^a National Engineering Research Center for Nanomedicine, Huazhong University of Science and Technology, Wuhan City, PR China

^b College of Life Science and Technology, Huazhong University of Science and Technology, Wuhan City, PR China

^c Interventional Radiology Department of Wuhan Union Hospital, Huazhong University of Science and Technology, Wuhan City 430022, PR China

ARTICLE INFO

Article history:

Received 17 January 2013

Received in revised form 18 June 2013

Accepted 13 August 2013

Available online 22 August 2013

Keywords:

Pickering emulsion

Temperature/pH-sensitive

Nanogel

Drug loading

Sustained release

ABSTRACT

pNIPAM nanogels, which exhibited rich sol–gel transition behavior, have been used extensively in the biomedical fields such as drug delivery, blood vessel embolization and tissue-engineering. Owing to their limitation of 3D networks, pNIPAM nanogels have low drug-loading amount and poor sustained releasing properties. In the present research, Pickering emulsion combined with solvent evaporation (PESE) is developed firstly as a new drug-loading technique of pNIPAM nanogels in our knowledge. The entrapment efficiency (EE%) reached nearly 100%, and DOX loading amount (DL%) could reach 15%. Owing to ionic bonding interaction of DOX molecules and sulfonamide groups, DOX loaded PNS nanogels by PESE (PNS-D nanogels) show a slow releasing behavior, only 13.2% for 48 h in pure water, without any burst release. As the ionic strength of media increased, the DOX-releasing amount from PNS-D-10 nanogels increased to 29.5%, 41.6% and 48.0% respectively in 0.9 wt%, 3.0 wt% and 5.0 wt% of NaCl solutions for 48 h. The loading DOX has significant effect on the rheologic behavior of nanogel dispersions. PESE technique is hopeful to be developed as a universal hydrophobic drug loading method of nanogels, and will be extensively applied in drug delivery and tissue engineering.

© 2013 Elsevier Ltd. All rights reserved.

1. Introduction

The temperature-responsive p(N-isopropylacrylamide) (pNIPAM) nanogels have been widely used as drug vehicles [1], biosensing [2] and tissue-engineering scaffold materials [3]. Moreover, multi-stimuli responsive nanogels could be developed by incorporation of functional monomers (e.g. acrylic acid), inorganic and metal nanoparticles (such as Fe₃O₄, Au and Ag nanoparticles) [4–6]. Compared to linear pNIPAM polymers, pNIPAM nanogels with nanometer-sized polymeric networks have unique microtopological structure, and exhibit much richer sol–gel phase transition behavior [7,8]. For example, concentrated pNIPAM nanogel dispersions showed three phase states (swollen gel, flowable sol and shrunken gel) with the increasing temperature from 10 °C to 40 °C. Based on their temperature sensitive sol–gel transition, Con-

centrated pNIPAM nanogels has been developed as a blood–vessel-embolic materials with good flowability and high mechanical strength in transcatheter arterial embolization (TAE) therapy of liver tumors in our recent research [9].

In order to improve therapeutic effect of tumors, many chemotherapeutic drugs (such as doxorubicin, paclitaxel, 5-fluorouracil) was often used in combination with TAE, namely transcatheter arterial chem-embolization (TACE) [10]. Unfortunately, the curative effect of TACE was limited by the low drug-loading amount and poor sustained release of embolic materials. Recently many nanomedicines (such as liposome, micelles, solid lipid nanoparticles and polymeric nanoparticles), which have many advantages including high loading capacity, good controlled release and biocompatibility etc., has been broadly applied in diagnosis and therapy of tumors [11–14]. Most of polymeric nanoparticles, such as polymeric micelle and dendrimer, could be co-dissolved first with hydrophobic drugs in an organic solvent, and then the polymer and drug were co-precipitated in an aqueous solution after removing organic solvent, that is, so-called emulsion solvent evaporation [15]. Being insoluble in any organic solvent, however, pNIPAM nanogels could not load drug by emulsion solvent evaporation method. In fact, the most common method is physic absorption for the drug-loading of pNIPAM nanogels. For this reason, pNIPAM

* Corresponding author at: National Engineering Research Center for Nanomedicine, Huazhong University of Science and Technology, Wuhan City, PR China. Tel./fax: +86 27 68789303, tel./fax: +86 27 87792147.

E-mail addresses: zhaoyb@mail.hust.edu.cn, zhaoyb@hust.edu.cn (Y. Zhao).

¹ Tel./fax: +86 27 68789303.

² Tel./fax: +86 27 87792147.

³ Tel./fax: +86 27 87792234.

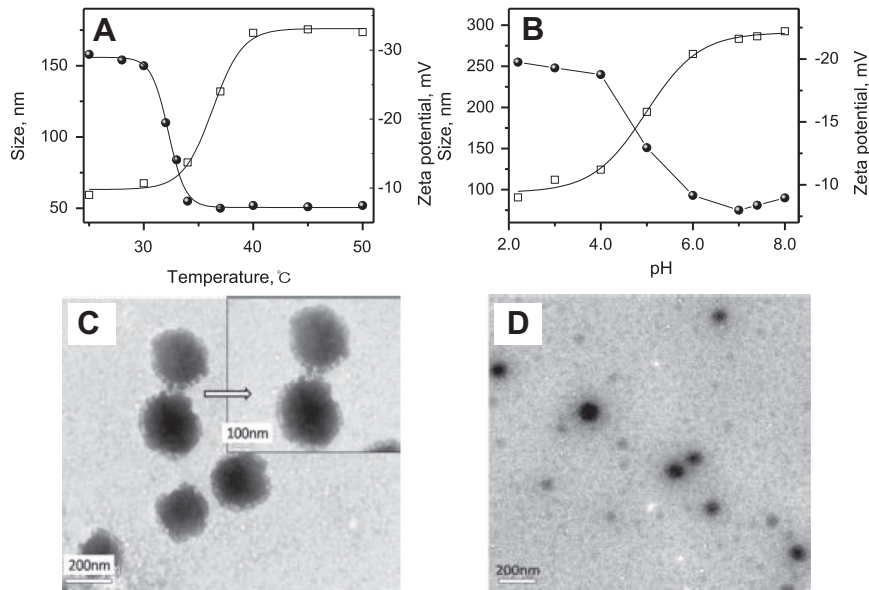


Fig. 1. The size (solid sphere) and zeta potential (hollow square) curves of PNS nanogel as a function of temperature (Plot A) and pH (Plot B); TEM images of PNS nanogel dried under 25 °C (Plot C) and 37 °C (Plot D).

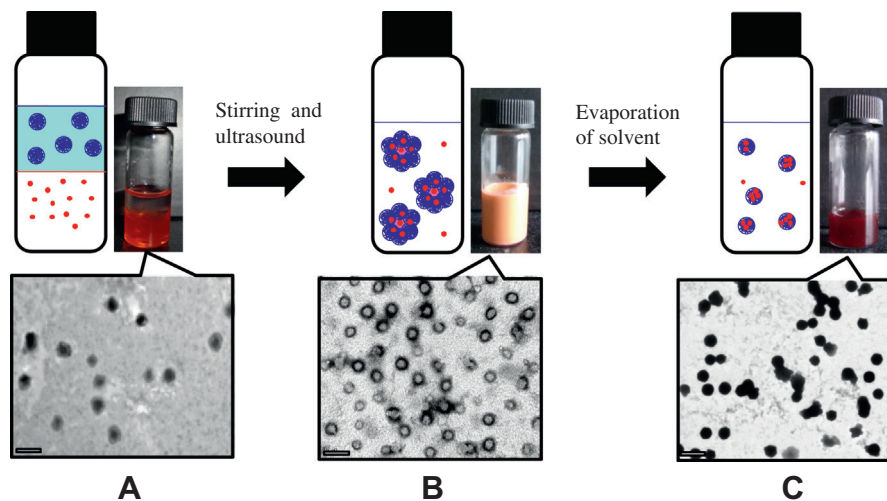


Fig. 2. The schematic diagram of the DOX-loading process of PNS nanogel by the Pickering emulsion evaporation technology. (A) the TEM picture of PNS nanogels before Pickering emulsification; (B) the TEM picture of emulsion drops stabilized by PNS nanogels and (C) the TEM picture of PNS-D nanogels after solvent evaporation. The scale is 500 nm.

Table 1

The drug loading amount (DL%) and the entrapment efficiency (EE%) of PNS and PNS-D nanogels.

	Z-average Size (nm, 25 °C)	PDI (25 °C)	The loading method	EE (%)	DL (wt%)
PNS nanogel	208	0.25	PA ^a	36.2 ± 7.2	1.3 ± 0.2
PNS nanogel	224.5	0.18	SD ^b	68.2 ± 1.6	5.23 ± 0.06
PNS-D-05	235	0.27	PESE ^c	98.7 ± 0.6	4.70 ± 0.03
PNS-D-10	294.8	0.28	PESE	99.0 ± 0.6	9.00 ± 0.05
PNS-D-15	489	0.31	PESE	99.1 ± 0.3	12.93 ± 0.04

^a Physical absorption: the mixing solution of DOX and nanogels were stirred overnight, and then dialyzed for removing the free DOX.

^b Solvent diffusion method: the DMSO solution of DOX and nanogels was added dropwise to water.

^c Pickering emulsion solvent evaporation.

nanogels were limited to the loading of hydrophilic drugs. Moreover, an initial burst release was often found in pNIPAM nanogels by physic absorption method.

Pickering emulsion, which was first reported by Pickering [16] and Ramsden [17] about a century ago, was an emulsion that is sta-

bilized solely by solid, mostly inorganic nano/micro-particles in the common sense. Its emulsified mechanism involved in the three-phase contact angle θ , which determined the particle position in the oil–water interface. Recently, several groups found that stimuli-responsive Pickering emulsion could be stabilized by some

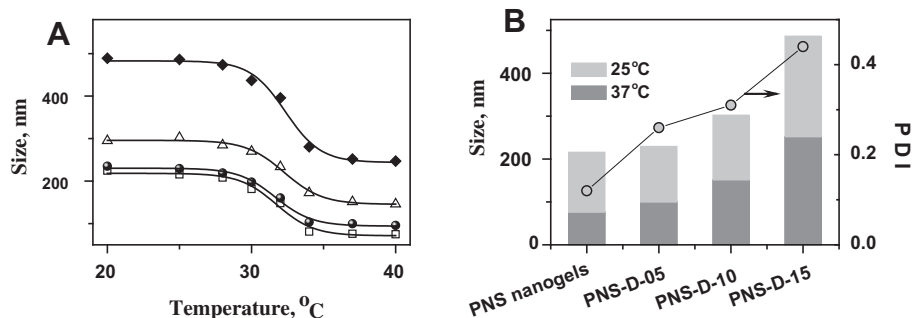


Fig. 3. (A) The size of PNS-D nanogels as a function of temperature in plot A. PNS nanogel (hollow square); PNS-D-05 nanogel (solid sphere); PNS-D-10 nanogel (hollow triangle); PNS-D-15 (solid diamond) and (B) the influence of the DOX-loading amount of PNS nanogels on the size and size distribution (polydispersity index, PDI). The PDI data was measured at 25 °C.

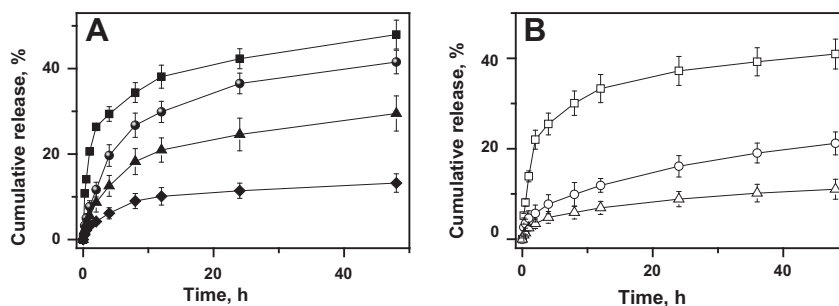


Fig. 4. (A) The influence of NaCl concentration on *in vitro* release of DOX from PNS-D-10 nanogel dispersions. 0 wt% (solid diamond), 0.9 wt% (solid triangle), 3 wt% (solid sphere), 5 wt% (solid square) and (B) the influence of pH on *in vitro* release of DOX from PNS-D-10 nanogel dispersions. pH 5.0 (hollow square), pH 6.0 (hollow sphere), pH 7.4 (hollow triangle).

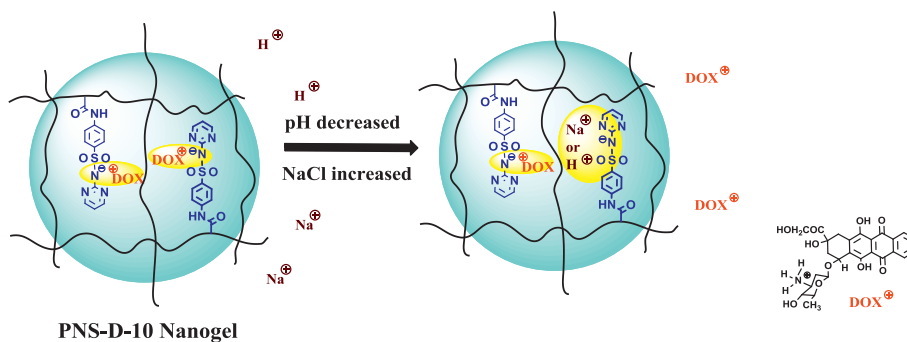


Fig. 5. The releasing mechanism of DOX from PNS-D nanogel.

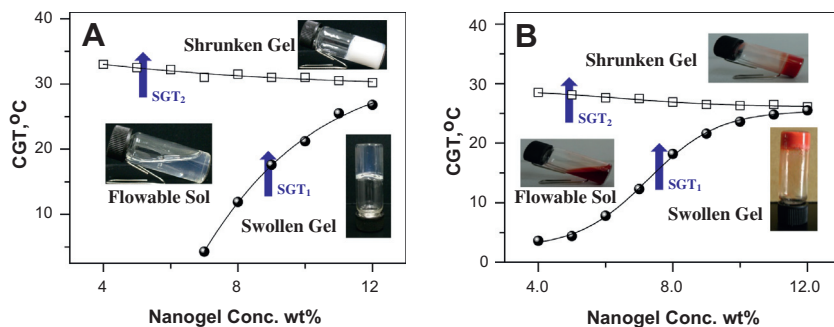


Fig. 6. The temperature sensitive sol-gel phase transition diagrams of both concentrated dispersions of PNS nanogels (A) and PNS-D-10 nanogels (B). The nanogel concentration was 10 wt%.

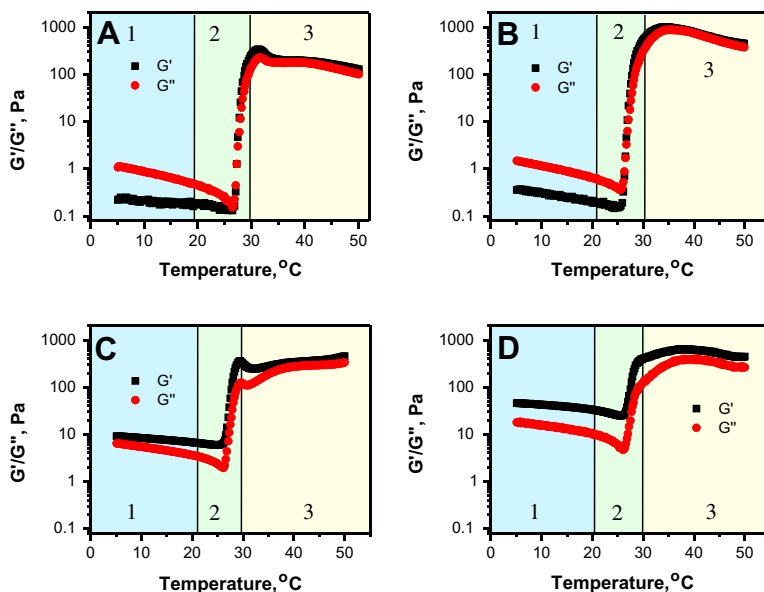


Fig. 7. The dynamic viscoelastic behavior of PNS-D nanogel dispersions: PNS nanogel dispersion (A); PNS-D-5 nanogels dispersion (B); PNS-D-10 nanogels dispersion (C); PNS-D-15 nanogels dispersion (D). The nanogel concentration was 10 wt%. Area 1, 2, 3 were represented swollen gel, flowable sol and shrunken gel respectively.

soft particles like “smart” nanogels/microgels, and evolved “on demand” under external stimuli such as temperature, pH, and magnetic field [18–20]. Veronique Schmitt group’s research and our previous work suggested that the deformability of soft nanogels and the interfacial rheologic properties had more important influence on the emulsion stability, rather than the three-phase contact angle θ [21,22]. Until now, Pickering emulsion technique has been mostly used to construct supracolloidal structures, such as permeable hollow capsules, colloidosomes, complex gels, and Janus particles [23,24]. Despite of many advantages such as surfactant-free, more stable and higher internal phase ratio, it was surprising in our knowledge that Pickering emulsion has been seldom reported in the application in encapsulation and transport of drugs.

In the present work, the O/W-type Pickering emulsion was stabilized only by dual temperature/pH-sensitive poly(N-isopropylacrylamide-co-methacrylate sulfadiazine) nanogel (PNS nanogel). After removing oil phase, hydrophobic Doxorubicin (DOX, an anti-tumor drug) dissolved in oil phase could be deposited into the network of PNS nanogels. Similar to common emulsion–solvent-evaporation method in the drug-loading of many nanomedicines, this drug-loading method was designated as Pickering emulsion solvent evaporation (PESE) method. We investigated the aggregation behavior of PNS nanogels in Pickering emulsion process by TEM. The drug loading amount (DL%), the entrapment efficiency (EE%) and *in vitro* releasing behavior of PNS nanogels by PESE method were compared with that by other methods. In order to the application on injectable hydrogel drug delivery or blood–vessel-embolic materials, concentrated PNS nanogel dispersions have been studied on their rheologic behavior.

2. Experimental

2.1. Materials

N-isopropylacrylamide (NIPAM, purity > 98.0%, Tokyo Chemical Industry Co., Ltd., Japan) and N,N'-methylenebisacrylamide (BIS, purity \geq 98.0%, Kermel Chemical Industry Co., Ltd., China) were recrystallized from n-hexane (purity \geq 97.0%, Sinopharm Chemical Reagent Co., Ltd., China) and methanol (purity \geq 99.5%, Sinopharm Chemical Reagent Co., Ltd., China), respectively. Methacryloyl

chloride (purity \geq 97.0%, Sigma–Aldrich Co., Ltd., USA), sulfadiazine (purity \geq 99.0%, Sigma–Aldrich Co., Ltd., USA), Sodium dodecyl sulfate (SDS, purity \geq 86.0%, Kermel Chemical Industry Co., Ltd., China), potassium persulfate (KPS, purity \geq 99.5%, Kermel Chemical Industry Co., Ltd., China) were used directly without further purification. NaOH (purity \geq 96.0%, Sinopharm Chemical Reagent Co., Ltd., China), HCl (36.0–38.0%, Sinopharm Chemical Reagent Co., Ltd., China), Chloroform (purity \geq 99.0%, Sinopharm Chemical Reagent Co., Ltd., China), acetone (purity \geq 99.5%, Sinopharm Chemical Reagent Co., Ltd., China), Triethylamine (purity \geq 99.0%, Aladdin Reagent Co., Ltd., Shanghai city, China) were commercially available. Milli-Q ultra-pure water was used in all experiments. Doxorubicin hydrochloride (DOX-HCl, purity > 98.0%) was purchased from Zhejiang Hisun Pharmaceutical Co., Ltd., China.

2.2. The synthesis of methacrylate sulfadiazine (MSD)

Methacrylate sulfadiazine (MSD) was synthesized according to modified Bae’s method [25]. In brief, sulfadiazine (25 g, 100 mmol) and NaOH (8 g, 200 mmol) were dissolved in 150 mL of acetone/water (60/90 v/v) mixture solution. In the resulting kelly solution, methacryloyl chloride (15 mL, 155 mmol) was added dropwise with stirring in ice salt bath. After reacting for 3.0 h in dark, the solution was adjusted to pH 5.0–6.0 by HCl solution (0.01 mol/L). The precipitated product was collected by filtration and washed three times with distilled water. The yellowish green solid (31 g, 97%) was obtained after drying in vacuum at 40 °C for 3 h. ^1H NMR (400 MHz, d_6 -DMSO): δ = 1.95 (3H, $-\text{CH}_3$), 5.5 (1H, $=\text{CH}_2$), 5.8 (1H, $=\text{CH}_2$), 7.8–8.0 (4H, $-\text{C}_6\text{H}_4-$), 8.0–8.5 (3H, $-\text{C}_4\text{N}_2\text{H}_3-$), 10.1 (1H, $-\text{CONH}-$), 11.6 (1H, $-\text{SO}_2\text{NH}-$).

2.3. The preparation of PNS nanogel

Poly(N-isopropylacrylamide-co-methacrylate sulfadiazine) (PNS) nanogel was prepared by precipitation polymerization [9]. In brief, NIPAM (10.0 g, 88.4 mmol), MBA (0.1 g, 0.6 mmol), MSD (2.4 g, 7.5 mmol) and SDS (0.27 g, 0.92 mmol) were dissolved in NaOH solution (1.5 mg/mL, 800 mL). The resulting solutions were degassed for at least 60 min by bubbling N_2 and heating to 70 °C

under stirring. KPS (0.4 g, 1.5 mmol) was then added as polymerization initiator, and the reaction was maintained under an N₂ atmosphere at 70 °C for 5.0 h. The resulting PNS nanogels were dialyzed (the cutoff molecular weight is 14,000 Da) against water for 2 weeks to remove unreacted monomers and other small molecules. PNS nanogels were lyophilized and stored in a desiccator at room temperature.

2.4. The preparation of Pickering emulsion stabilized by PNS nanogels

Chloroform (1 mL) and Triethylamine (TEA, 5.0 μL) were added into PNS nanogel dispersion (1.0 wt%, 3 mL). The preliminary emulsion was obtained after shearing the mixture at 13,000 rpm in ice-water bath for 10 min (FA25 homogenizer, FLUKO Equipment Shanghai Co., Ltd., China). The stable Pickering nano-emulsion was prepared by ultrasonication of the preliminary emulsion using an ultrasonic cell disruptor (JY92-IIN, 800 W, 20–25 kHz, Ningbo Scientz Biotechnology Co., Ltd., China). The diameter of the ultrasonic amplitude transformer is 2 mm. In order to avoid too high temperature caused by ultrasonication for long time, the emulsion was in ice bath, and the interval time was set as 5 s after 5 s of working time. The total working time was 75 s.

2.5. The preparation of Doxorubicin-loaded PNS nanogels (PNS-D nanogels)

Pickering emulsion solvent evaporation (PESE) method was developed for the preparation of Doxorubicin-loaded PNS nanogels (PNS-D nanogels). According to the feeding ratio of Doxorubicin and nanogel, PNS-D nanogels were designated as PNS-D-15, PNS-D-10, PNS-D-05, respectively. For example, PNS-D-15 was prepared as follows: DOX-HCl (4.5 mg, 7.8×10^{-3} mmol) was dissolved in Chloroform (1 mL, containing 5.0 μL TEA). The solution was added into PNS nanogel dispersion (1.0 wt%, 3 mL), and then was emulsified to a preliminary emulsion in ice-water bath by shearing at 13,000 rpm for 10 min. The stable Pickering nano-emulsion was prepared by also ultrasonication of the preliminary emulsion according to above ultrasonication condition. After removing chloroform by a rotatory evaporator, the resulting PNS-D nanogel dispersion was lyophilized and stored in dark.

2.6. Characterization

The hydrodynamic diameters and the zeta potentials of PNS nanogels and the emulsion droplet were determined by dynamic light scattering (DLS, Zetasizer Nano-ZS 90, Malvern Instrument Limited, UK) using a He-Ne laser source ($\lambda = 633$ nm) with the scattering angle of 90°. All samples were diluted with ultrapure water to 0.5 mg mL⁻¹. The micromorphology of nanogels and emulsion droplets were characterized by Transmission Electron Microscope (TEM, Tecnai G2 20, FEI Corp., Netherlands) at 180 kV. A drop of nanogel dispersion or Pickering emulsion was added onto a carbon-coated copper grid, and then dried in air. The samples were negatively stained with 1 wt% phosphotungstic acid solution. The sol-gel phase transitions were measured by the inverting-vial method from 5 °C to 50 °C in water bath. The dynamic viscoelastic properties of nanogel dispersions were obtained using a strain-controlled rheometer (ARES-G2, TA Instruments-Waters LLC, USA) with a parallel plate ($\Phi = 40$ mm, gap set at 0.9 mm) in the range of 20–40 °C with following parameters: strain was 0.2%, heating rate was 1 °C min⁻¹, and frequency was 1.0 Hz.

2.7. Drug loading and in vitro releasing behavior

In order to determine the drug loading amount and the entrapment efficiency of PNS-D nanogel dispersions, PNS-D nanogel dis-

persions (0.25 wt%, 1.5 mL) were added into a ultrafiltration tube (Minipore, MwCO 10 K, 4 mL), and then centrifuged (3000 rpm, 1.0 h). The resulting supernatant was diluted 200-fold, and free DOX was measured by fluorospectrophotometry (F4500, Hitachi Co., Japan). The measured condition was: $\lambda_{\text{ex}} = 500$ nm, $\lambda_{\text{em}} = 556$ nm, PMT Voltage = 700 V. The drug loading amount (DL%) and the entrapment efficiency (EE%) were calculated respectively as following:

$$\text{DL}\% = \frac{W_0 - C_f \cdot V_f}{C_n \cdot V_n} \quad (1)$$

$$\text{EE}\% = \frac{W_0 - C_f V_f}{W_0} \quad (2)$$

Here, W_0 is the feeding amount of DOX, C_f and V_f is the concentration and volume of free DOX, respectively. C_n and V_n is the concentration and volume of nanogel dispersion.

3. Results and discussion

3.1. The preparation of poly(*N*-isopropylacrylamide-co-methacrylate sulfadiazine) (PNS) nanogel

Sulfonamide, a well known antibacterial agent, has been used recently as a new pH-sensitive group due to its weak acidic nature ($\text{p}K_a = 6.5\text{--}7.0$) [25–27]. Some antitumor drug carriers, which based on the pH-sensitivity of sulfonamide, have been constructed since most solid tumors have lower extracellular pH (<6.8) than their surrounding tissues and blood (pH 7.4) [28–30]. In the present work, PNS nanogels were prepared by precipitation copolymerization of NIPAM and resultant MSD monomer. From Fig. 1 A, the size of PNS nanogel decreased from 158 nm at 25 °C to 50 nm at 50 °C, and the zeta potential increased from -9 mV at 25 °C to -32.6 mV at 50 °C. Just like pNIPAM nanogels (classic temperature sensitive nanogels [9]), PNS nanogels exhibit a sudden change in size and zeta potential as temperature increased, that is, so called volume-phase transition. Its volume-phase transition temperature (VPTT) was about 32–35 °C. Fig. 1B exhibited the pH-sensitivity of PNS nanogel. With the increasing pH, the size of PNS nanogel decreased from 255 nm at pH 2.2 to 90 nm at pH 8.0, and the zeta potential increased from -9 mV at pH 2.2 to -22.2 mV at pH 8.0. The TEM pictures (Fig. 1C and D) showed that PNS nanogels were spherical and hairy morphology. All of these data indicated that PNS nanogels were highly deformable under the external stimuli such as temperature and/or pH.

3.2. The drug loading of PNS nanogels using Pickering emulsion solvent evaporation (PESE)

Due to their stimuli-responsive deformability, soft pNIPAM nanogels have been extensively applied as novel emulsifier, and the resultant Pickering emulsion can evolve “on demand” under some external stimuli, such as temperature, pH, and magnetic field [21]. Based on the emulsifying ability of pNIPAM nanogels, Pickering emulsion solvent evaporation (PESE) technology was developed as a new drug loading method as shown in Fig. 2. In our previous works, we found that an unstable emulsion (preliminary emulsion) which size was in 1.0–5.0 μm was formed by shearing the mixture of oil phase and aqueous nanogel dispersion phase at 13,000 rpm. The nanogels accumulated on O/W interfaces to form interfacial hydrogel layers. The interfacial hydrogel layers surrounding oil droplets, which form capsule-like microscopic suprastructures, provided strong interfacial hindrance to resist droplet-droplet coalescence. After further dispersed by ultrasound (strong energy input), the microscopic suprastructures were disin-

tegrated into the same capsule-like nanoscale suprastructures with near monodispersity (Fig. 2B). It is noteworthy that the nanoscale suprastructures has the same size as PNS nanogels (about 200 nm). As suggested in our previous works [22], input of ultrasound energy might trigger the dehydration of nanogels and make PNS nanogels shrunken. The shrunken nanogels absorbed on the oil/water interface, and decreased interfacial tension by covering on larger area of oil/water interface owing to its deformability. Consequently the nano-emulsion stabilized by PNS nanogels was very stable, and sustained unchanged in size and morphology for several days (Fig. 2B).

At last, the hollow oil-in-water droplets (Fig. 2B) were changed to solid nanoparticles (Fig. 2C) after removing chloroform by rotary evaporation. It was obvious that PNS nanogels were re-dispersed in water due to the remove of chloroform, and hydrophobic DOX was transferred into the 3D networks of PNS nanogels. In this process, the properties of droplets have important effect on the drug-loading of PNS nanogels. The inhomogeneous droplets of preliminary emulsion became unstable, and resulted in the precipitation of DOX and nanogels in solvent evaporation process.

As shown in Table 1, three stable PNS-D nanogel dispersions (PNS-D-05, PNS-D-10 and PNS-D-15) were prepared using PESE method. Fig. 3A showed that the sizes of three PNS-D nanogels have the same temperature dependence as PNS nanogels. That is, all PNS-D nanogels exhibited a significant drop in size (volume phase transition) with the increasing temperature, and their VPTTs were about 32–35 °C. It indicated that the loading DOX had nearly no influence on their VPTTs. Fig. 3B showed the influence of DOX-loading amount on the size and polydispersity index (PDI) of PNS-D nanogels. Their sizes increased as the DOX-loading amount increased at either 25 °C or 37 °C. With the increase of DOX-loading amount, the PDIs of PNS-D nanogels also increased from 0.12 (PNS nanogels) to 0.44 (PNS-D-15 nanogels). It was likely to be because hydrophobic DOX molecules resulted in the aggregation of PNS-D nanogels, which decreased the stability of nanogel dispersions. When the feeding ratio of DOX and nanogels was higher than 0.15, in fact, stable PNS-D nanogel dispersions could be not prepared using PESE method owing to the precipitation of DOX and nanogels.

The drug loading amount (DL) and the entrapment efficiency (EE) are two important parameters in the evaluation of drug-loading capability. As shown in Table 1, PNS nanogels could reach higher DL value by solvent diffusion method. However, low EE value indicated that a large amount of DOX was not encapsulated in PNS nanogels. It could be attributed to the fact that a large amount of DOX molecules migrated into water in the diffusion of DMSO to water. Compared with the common drug-loading technology of nanogels, such as the solvent diffusion and the physical absorption, PNS nanogels had higher DL and EE values using PESE technology. Near 100% of EE value showed that all DOX molecules were migrated into the 3D networks of PNS nanogels, and the highest DL value arrived at about 15 wt%.

3.3. *In vitro* sustained releasing behavior of PNS-D nanogels

Recent studies suggested that sustained drug release could improve local DOX-concentration in tumor tissue and reduce its systemic concentration in TACE therapy. For example, drug-eluting beads (DEBs) such as DC Bead™ and QuadraSphere™ remained much higher DOX concentration in tumor tissue up to 14 days, whereas systemic drug concentration is kept at minimal level [31–35]. Similarly with these drug-eluting beads, PNS-D-10 nanogels exhibited a slow release without any burst release. Their cumulative release only reached 13.2% for 48 h (Fig. 4A), and about 76.8% of DOX-loading amount could be not released in pure water. As the ionic strength of media increased, however, the DOX-releas-

ing amount increased from PNS-D-10 nanogels. At 48 h, their releases reached 29.5%, 41.6% and 48.0% respectively in 0.9 wt%, 3.0 wt% and 5.0 wt% of NaCl solutions (Fig. 4A). It indicated that PNS-D-10 nanogels showed a controlled slow but constant release in salt solution.

PNS-D-10 nanogels showed a pH dependence of *in vitro* DOX release as shown in Fig. 4B. Similarly with its release in pure water, the cumulative release of DOX was very low (only 11.0% for 48 h) for PNS-D-10 nanogels at pH 7.4 (the pH value of normal tissues and blood). It indicated that PNS-D-10 nanogels induced little systemic toxicity due to their small release in blood. As the pH of media decreased, the release of DOX from PNS-D-10 nanogels increased, for example, its release reached up to 40% for 48 h at pH 5.0. It was noteworthy that PNS-D-10 nanogels showed a slow and constant release at pH 6.0 (the pH value of tumor tissues). Their DOX-releasing amount reached 21.1% for 48 h, and still persistently increased with the increase of releasing time. The results suggested that PNS-D-10 nanogels could maintain a sustained drug release in tumor tissue, which resulted in the improvement of DOX concentration in tumor tissue and the enhancement of therapeutic efficacy for tumors.

As shown in Fig. 5, the ionic bonding interaction between DOX molecules and sulfonamide groups of PNS nanogel networks could be responsible for the pH- and/or ion-dependent release. The tight complex by ionic bonding interaction between DOX molecules and sulfonamide groups resulted in the slow release of PNS-D-10 nanogels at pH 7.4. As pH decreased or ionic strength increased, the ionic bonding interaction was broken due to the ionizing of DOX molecules. Therefore, free DOX molecules were released from the networks of PNS-D-10 nanogels.

3.4. The sol-gel phase transition behavior of PNS nanogel

The sol-gel phase transition behavior of PNS and PNS-D-10 nanogel dispersions was shown in Fig. 6. With the increasing temperature and nanogel concentration, both nanogel dispersions successively exhibited three phase states: swollen gel, flowable sol and shrunken gel, in according with our previous works [6]. Therefore, there were two sol-gel phase transition temperatures (SGT1 and SGT2), which were corresponding respectively to the transition from swollen gel to flowable sol and the transition from flowable sol to shrunken gel. The SGT1 increased as the nanogel concentration increased. However, the nanogel concentration has nearly no influence on the SGT2. It could be attributed to the different gelating mechanism. The swollen gel was formed by the volume blocking mechanism according to the hardsphere theory [36,37], while the shrunken gel was formed due to the enhanced interaction (hydrophobic force and electrostatic force) between nanogel particles, in accordance with the softsphere theory [38].

The DOX loading amount has different influence on the two sol-gel phase transition. The SGT1 value obviously increased after DOX loading by the PESE method. For example, the SGT1 value increased from 11.9 °C of PNS nanogels to 18.2 °C of PNS-D-10 nanogels at 8.0 wt%. This could be attributed to the fact that the loading DOX made nanogel size increased as shown in Fig. 3. Therefore, the swollen gel could occur at higher temperature. On the other hand, the SGT2 value has slightly decreased (e.g. from 31.5 °C of PNS nanogels to 26.9 °C of PNS-D-10 nanogels at 8.0 wt%). It was because that the loading DOX by PESE method enhanced hydrophobic interaction of nanogel particles.

The influence of DOX on the viscoelastic behavior of concentrated PNS-D-10 dispersions was characterized by a strain-controlled rheometer in Fig. 7. Four nanogel dispersions had the similar viscoelastic behavior. That is, the G' and G'' values were low below 25 °C, increased abruptly at the range of 28–30 °C, and slightly decreased above 30 °C. Area 1, 2 and 3 represented

swollen gel, flowable sol and shrunken gel respectively. In swollen gel (area 1), the size of PNS nanogels decreased with the increasing temperature. According to volume blocking mechanism of hard-sphere theory, the reduction in size led to the drop in gel strength of PNS-D nanogels. When the gel strength decreased further as temperature increased, swollen gel turned into flowable sol (area 2). As temperature increased above the VPTTs of PNS nanogels, the inter-particle forces (hydrophobic interaction and electrostatic force) between nanogels enhanced abruptly. It made the G' and G'' value increased, and indicated the transition from flowable sol to shrunken gel (area 3). According to soft-sphere theory [38], colloid gelation was controlled by the equilibrium of attractive and repulsive force between colloid particles. A attractive hydrophobic attraction and electrostatic repulsion were enhanced simultaneously due to the hydrophilic/hydrophobic transition and the change of zeta potential of PNS nanogels in the transition from flowable sol to shrunken gel. Since the DOX loading could increase the nanogel size, but do not change the inter-particle force, the G' and G'' value of swollen gel increased with the increasing amount of DOX, and that of the shrunken gel has been little changed, as shown in Fig. 7.

4. Conclusion

A temperature/pH-sensitive nanogel was synthesized by precipitation polymerization. A new drug-loading method, Pickering emulsion-solvent evaporation (PESE), was developed for hydrophobic drug loading of PNS nanogels. The entrapment efficiency (EE%) reached nearly 100%, and the DOX loading amount (DL%) could reach 15%. DOX loaded PNS nanogels by PESE (PNS-D nanogels) showed a slow releasing behavior, without any burst release. Moreover, PNS-D-10 nanogels showed a pH dependence of *in vitro* DOX release. The ionic bonding interaction of DOX molecules and the sulfonamide groups could be responsible for the pH-dependence. PNS-D nanogel dispersion showed three phase states (swollen gel, flowable sol and shrunken gel) with the increasing temperature. Due to sol–gel phase transition behavior and sustained drug release with pH-sensitivity, PNS nanogels could be helpful to be developed as injectable hydrogel carriers or blood-embolic materials for interventional therapy of some solid tumors.

Acknowledgements

This work was financially supported by the grant from National Basic Research Program of China (973 Program, 2012CB932500), National High Technology Research and Development Program of China (SS2012AA023804), and the National Science Foundation of China (NSFC, 31170960/C1007). We also thank the Analysis and Test Center of Huazhong University of Science and Technology for the related analysis.

References

- [1] R.L. Bartlett II, M.R. Medow, A. Panitch, B. Seal, *Biomacromolecules* 13 (2012) 1204–1211.
- [2] W.J. Lin, X.M. Ma, J.S. Qian, A.I. Abdelrahman, A. Halupa, V. Baranov, A. Pich, M.A. Winnik, *Langmuir* 27 (2011) 7265–7275.
- [3] Z.Y. Shen, J.X. Bi, B.Y. Shi, D. Nguyen, C.J. Xian, H. Zhang, S. Dai, *Soft Matter* 8 (2012) 3250–3257.
- [4] D. Suzuki, H. Kawaguchi, *Langmuir* 22 (2006) 3818–3822.
- [5] G.Z. Wang, Y. Zhang, Y. Fang, Z.Z. Gu, *J. Am. Chem. Soc.* 90 (2007) 2067–2072.
- [6] T. Hoare, R. Pelton, *Macromolecules* 37 (2004) 2544–2550.
- [7] G. Romeo, A. Fernandez-Nieves, H.M. Wyss, D. Acierno, D.A. Weitz, *Adv. Mater.* 22 (2010) 3441–3445.
- [8] B.H. Tan, R.H. Pelton, K.C. Tam, *Polymer* 51 (2010) 3238–3243.
- [9] Y. Zhao, C. Zheng, Q. Wang, J. Fang, G. Zhou, H. Zhao, Y. Yang, H. Xu, G. Feng, X. Yang, *Adv. Funct. Mater.* 21 (2011) 2035–2042.
- [10] S. Gupta, K.C. Wright, J. Ensor, C.S.V. Pelt, K.A. Dixon, V. Kundra, *Cardiovasc. Interv. Radiol.* 34 (2011) 1021–1030.
- [11] R.K. Jain, T. Stylianopoulos, *Nat. Rev. Clin. Oncol.* 7 (2010) 653–664.
- [12] E. Fleige, M.A. Quadir, R. Haag, *Adv. Drug Deliver. Rev.* 64 (2012) 866–884.
- [13] J. Croissant, J.I. Zink, *J. Am. Chem. Soc.* 134 (2012) 7628–7631.
- [14] F. Rossella, C. Soldano, V. Bellani, M. Tommasini, *Adv. Mater.* 24 (2012) 2453–2458.
- [15] R. Lopes, C.V. Eleuterio, L.M.D. Goncalves, M.E.M. Cruz, A.J. Almeida, *Eur. J. Pharm. Sci.* 45 (2012) 442–450.
- [16] S.U. Pickering, *J. Chem. Soc. Trans.* 91 (1907) 2001–2021.
- [17] W. Ramsden, *Proc. Roy. Soc. London* 72 (1903) 156–164.
- [18] S. Fujii, E.S. Read, B.P. Binks, S.P. Armes, *Adv. Mater.* 17 (2005) 1014–1018.
- [19] T. Ngai, H. Auweter, S.H. Behrens, *Macromolecules* 39 (2006) 8171–8177.
- [20] B. Brugger, B.A. Rosen, W. Richtering, *Langmuir* 24 (2008) 12202–12208.
- [21] M. Destribats, V. Lapeyre, M. Wolfs, E. Sellier, F. Leal-Calderon, V. Ravaine, V. Schmitt, *Soft Matter* 7 (2011) 7689–7698.
- [22] H. Chen, H. Zhu, J. Hu, Y. Zhao, Q. Wang, J. Wan, Y. Yang, H. Xu, X. Yang, *ACS Nano* 5 (2011) 2671–2680.
- [23] M. Lattuada, T.A. Hatton, *Nano Today* 6 (2011) 286–308.
- [24] Z.W. Niu, J.B. He, T.P. Russell, Q.A. Wang, *Angew. Chem. Int. Ed.* 49 (2010) 10052–10066.
- [25] S.K. Han, K. Na, Y.H. Bae, *Colloid Surf. A* 214 (2003) 49–59.
- [26] W.S. Shim, S.W. Kim, D.S. Lee, *Biomacromolecules* 7 (2006) 1935–1941.
- [27] K. Dayananda, B.S. Pi, B.S. Kim, T.G. Park, D.S. Lee, *Polymer* 48 (2007) 758–762.
- [28] K. Na, K.H. Lee, Y.H. Bae, *J. Control. Release* 97 (2004) 513–525.
- [29] V.A. Sethuraman, K. Na, Y.H. Bae, *Biomacromolecules* 7 (2005) 64–70.
- [30] L. Liu, P. Jin, M. Cheng, G. Zhang, F. Zhang, *Chem. Eng. J.* 14 (2006) 377–382.
- [31] K.-H. Lee, E. Liapi, C. Cornell, P. Reb, M. Buijs, J. Vossen, V. Ventura, J.-F. Geschwind, *Cardiovasc. Interv. Radiol.* 33 (2010) 576–582.
- [32] A. Lewis, M. Gonzalez, S. Leppard, J. Brown, P. Stratford, G. Phillips, A. Lloyd, *J. Mater. Sci. – Mater. Med.* 18 (2007) 1691–1699.
- [33] M. Gonzalez, Y. Tang, G. Phillips, A. Lloyd, B. Hall, P. Stratford, A. Lewis, *J. Mater. Sci. – Mater. Med.* 19 (2008) 767–775.
- [34] A. Lewis, C. Adams, W. Busby, S. Jones, L. Wolfenden, S. Leppard, R. Palmer, S. Small, *J. Mater. Sci. – Mater. Med.* 17 (2006) 1193–1204.
- [35] K. Malagari, M. Pomoni, A. Kelekis, A. Pomoni, S. Dourakis, T. Spyridopoulos, H. Moschouris, E. Emmanouil, S. Rizos, D. Kelekis, *Cardiovasc. Interv. Radiol.* 33 (2010) 541–551.
- [36] C.G. de Kruijff, E.M.F. van Iersel, A. Vrij, W.B. Russel, *J. Chem. Phys.* 83 (1985) 4717–4725.
- [37] D.M. Öle Kiminta, P.F. Luckham, S. Lenon, *Polymer* 36 (1995) 4827–4831.
- [38] D. Gottwald, C.N. Likos, G. Kahl, H. Lowen, *J. Chem. Phys.* 122 (2005) 07493-1–07493-7.